Automatica 88 (2018) 48–56

Contents lists available at ScienceDirect

Automatica

journal homepage: www.elsevier.com/locate/automatica

Brief paper

An incremental harmonic balance-based approach for harmonic analysis of closed-loop systems with Prandtl–Ishlinskii operator[☆]

Lei Fang[a], Jiandong Wang[b,*], Xiaobo Tan[c]

[a] College of Engineering, Peking University, Beijing, China
[b] College of Electrical Engineering and Automation, Shandong University of Science and Technology, Qingdao, China
[c] Smart Microsystems Lab, Department of Electrical and Computer Engineering, Michigan State University, East Lansing, MI, USA

ARTICLE INFO

Article history:
Received 8 March 2016
Received in revised form 17 March 2017
Accepted 24 May 2017

Keywords:
Nonlinear system analysis
Harmonic response
Hysteresis
Incremental harmonic balance

ABSTRACT

Analyzing hysteretic systems presents a significant challenge due to the memory effect of hysteresis. In this paper we present an incremental harmonic balance (IHB)-based approach to compute the steady-state response of a closed-loop system with hysteresis under a sinusoidal excitation, where the hysteresis element is modeled by the Prandtl–Ishlinskii (PI) operator. While the describing function method (DFM) can be used to obtain an approximate solution for the closed-loop system based on first-order harmonics, the proposed IHB-based approach iteratively calculates the harmonic components of the hysteretic system up to an arbitrary order. The main challenge is the harmonic calculation of the periodic output of the PI operator for a multi-harmonic input. In order to address this problem, an alternative definition of the play operator is utilized as the hysteron for the PI operator. By using the alternative definition, a set of switching time instants, when the play operator enters or exits the boundary region, are determined by a bisection method. The calculation of the incremental harmonic components is finally reformulated as a linear matrix equality that can be solved efficiently. As an illustration, numerical results for a system involving a proportional–integral feedback controller are presented to demonstrate the advantage of the IHB-based approach over the DFM in approximating the harmonic response of the hysteretic system.

1. Introduction

Modeling and control of hysteretic systems has gained significant attention over the past several decades (Janaideh, Rakotondrabe, & Tan, 2016; Tan & Iyer, 2009). One reason for the rapid development is the wide application of smart materials, which exhibit considerable hysteretic behaviors (Bertotti & Mayergoyz, 2005; Smith, 2005). Another important reason is the hysteretic stiction from which many control valves in industrial processes suffer; as a result, modeling, detection, quantification, and compensation of control valve stiction have been active research topics recently (Choudhury, Shah, & Thornhill, 2008; Jelali & Huang, 2010). On the modeling side, one effective model for these systems takes a Hammerstein structure consisting of a hysteresis operator followed by a linear subsystem (Fang & Wang, 2015; Hsu & Ngo, 1997; Iyer & Tan, 2009). Several hysteresis operators are often adopted, including the Preisach operator (Tan & Baras, 2004), the Prandtl–Ishlinskii (PI) operator (Janaideh, Rakheja, & Su, 2009; Kuhnen, 2003), and the Preisach–Krasnosel'skii–Pokrovskii (PKP) operator (Riccardi, Naso, Janocha, & Turchiano, 2012; Webb, Lagoudas, & Kurdila, 1998), each of which is based on a weighted superposition of elementary hysteretic operators. On the control side, a popular control scheme is to construct an inverse hysteresis operator to compensate the hysteresis effect and to design a feedback controller to deal with the inversion error and remaining dynamics (Iyer & Tan, 2009; Kuhnen, 2003). In order to deal with sticky control valves, the knocker method (Hägglund, 2002), the constant reinforcement method (Ivan & Lakshminarayanan, 2009), the two-movement method (Cuadros, Munaro, & Munareto, 2012), and the controller tuning method (Mohammad & Huang, 2012) have been formulated.

Compared with the extensive work on modeling and control of systems with hysteresis, analysis for such systems is relatively limited (Cavallo, Natale, abd Pirozzi, & Visone, 2005; Edardar, Tan, & Khalil, 2014; Esbrook, Tan, & Khalil, 2014; Macki, Nistri, & Zecca, 1992). A major challenge is the memory effect, a key feature of

☆ This work was supported in part by the National Natural Science Foundation of China (No. 61061130559), Research Fund for the Taishan Scholar Project of Shandong Province of China, China Scholarship Council (No. 201406010203) and US National Science Foundation (CMMI 1301243). The material in this paper was partially presented at the 2016 American Control Conference, July 6–8, 2016, Boston, MA, USA. This paper was recommended for publication in revised form by Associate Editor Zongli Lin under the direction of Editor Daniel Liberzon.

* Corresponding author.
E-mail addresses: fanglei@pku.edu.cn (L. Fang), jiandong@sdust.edu.cn (J. Wang), xbtan@egr.msu.edu (X. Tan).

https://doi.org/10.1016/j.automatica.2017.11.005
0005-1098/

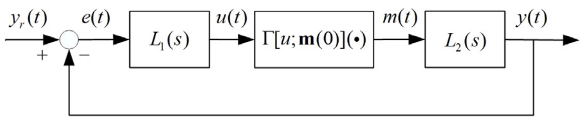

Fig. 1. Configuration of a nonlinear closed-loop system with hysteresis.

hysteresis, which results in complicated dynamic behaviors and significantly hinders the extension of analysis tools for systems with static nonlinearities (Brokate & Sprekels, 1996; Mayergoyz, 2003). An existing method for analyzing hysteretic systems is the describing function method (DFM) (Gelb & Velde, 1968), which utilizes the fundamental harmonic approximation of the periodic signals. However, the DFM is only effective when the hysteresis is weak; for systems with pronounced hysteresis, the accuracy of DFM drops quickly due to the influence of the higher-order harmonics (Mickens, 1984).

In this work, we present a novel approach to computing the frequency response of a closed-loop system with hysteresis. A key element of our approach is the extension of an incremental harmonic balance (IHB) method (Chen, Liu, & Meng, 2012; Shen, Yang, & Liu, 2006). The IHB method is an iterative algorithm, where the input to the nonlinearity of concern is assumed to consist of a series of harmonics, and the corresponding change in the output of the nonlinearity, due to an increment in the input harmonics, is computed via a first-order Taylor approximation. The IHB method has been used in analyzing systems with static nonlinearities, such as cubic polynomials (Chen et al., 2012) and dead zones (Shen et al., 2006); however, the memory effect of hysteresis makes the extension of the IHB method to hysteresis systems challenging. To the best of our knowledge, this paper is the first attempt to extend the IHB method to the harmonic analysis of hysteretic systems.

We consider the PI operator as the hysteresis model, which is a weighted superposition of multiple play operators. The PI operator and its extension have been widely utilized in control of hysteretic systems (Chen, Hisayama, & Su, 2009; Chen, Ren, & Zhong, 2016; Huang, Zhang, & Zhang, 2016; Janaideh & Kreji, 2013; Liu, Su, & Li, 2014; Riccardi, Naso, Turchiano, & Janocha, 2013; Shan & Leang, 2012; Wang & Su, 2006). The main challenge in extending the original IHB method to systems with a PI operator is the calculation of the periodic output of a PI operator for a multi-harmonic input. In order to address this problem, we exploit the results in Esbrook and Tan (2012), namely, the output of the play operator is described as a function of its input and a series of pulse waves determined by a set of switching time instants when the play operator enters or exits the interior region. With the switching time instants determined with a bisection method, the calculation of the incremental harmonic components is finally reformulated as a linear matrix equality that can be solved efficiently. Numerical results demonstrate that the performance of the proposed IHB-based approach is almost independent of the hysteresis severity, while the DFM deteriorates quickly as the hysteresis severity increases.

A preliminary study of this paper was presented as a conference paper (Fang, Wang, & Tan, 2016), where the hysteresis element is modeled by one single play operator. This paper extends the preliminary study to the PI hysteresis operator, so that the technical complexity is much higher. In addition, the proposed IHB-based approach is more complete, e.g., new steps are provided to determine the harmonic order.

The rest of this paper is organized as follows. Section 2 describes the problem to be solved. The details of the proposed IHB-based approach are presented in Section 3, while the DFM is briefly revisited in Appendix A. Numerical results are given in Section 4 to illustrate the effectiveness of the proposed approach. Concluding remarks are provided in Section 5.

2. Problem formulation

Consider a closed-loop system shown in Fig. 1, where a hysteresis operator $\Gamma[u;\mathbf{m}(0)](\cdot)$ is sandwiched by two linear components $L_1(s)$ and $L_2(s)$. Generally, $L_1(s)$ can represent a controller, while $L_2(s)$ may stand for the controlled linear dynamics. The signals $y_r(t)$, $e(t)$, $u(t)$, $m(t)$, and $y(t)$ denote the reference, control error, hysteresis input, hysteresis output, and system output, respectively. Here t is an nonnegative integer standing for the sampling index. In general, linear controllers are preferred owing to their simplicities in terms of design, parameter tuning and maintenance. Thus, more than 95% of industrial control loops use proportional–integral–differential controllers (Aström & Hägglund, 2006). When a hysteresis arises, e.g., when control valves become sticky as the time in service grows, a natural question is how much the performance of linear controllers is negatively affected by the hysteresis. If the effect is minor, then linear controllers are still preferred. To answer the question, a basic step is to perform some theoretical analysis including the harmonic analysis on the closed-loop system as represented in Fig. 1 with a linear controller $L_1(s)$.

The hysteresis Γ is assumed to be a classical PI operator consisting of a weighted superposition of basic hysterons called play operators. For a play operator P_r with an initial condition $m_r(0)$, when its input $u(t)$ is continuous and monotone, the output $m_r(t) = P_r[u; m_r(0)](t)$ is

$$P_r[u; m_r(0)](t) = \max\{\min\{u(t)+r, m_r(t-1)\}, u(t)-r\},$$

where $r > 0$ stands for the play radius. For a general continuous input, the input signal is broken into monotone segments, and the output is then calculated by setting the last output of one monotone segment as the initial condition for the next. Then, a finite-dimensional PI operator can be represented as

$$\Gamma[u;\mathbf{m}(0)](t) = \sum_{i=0}^{N} \theta_i P_{r_i}[u; m_i(0)](t) = \boldsymbol{\theta}^T \mathbf{P_r}[u;\mathbf{m}(0)](t), \qquad (1)$$

where the play radii of the $N+1$ play operators satisfy $0 = r_0 < r_1 < \cdots < r_N < \infty$, and θ_i is the weighting of the play operator P_{r_i}. Moreover, $\boldsymbol{\theta} \triangleq [\theta_0, \theta_1, \cdots, \theta_N]^T$, $\mathbf{r} \triangleq [r_0, r_1, \cdots, r_N]^T$, $\mathbf{m}(t) \triangleq [m_0(t), m_1(t), \cdots, m_N(t)]^T$, and $\mathbf{P_r} \triangleq [P_{r_0}, P_{r_1}, \cdots, P_{r_N}]^T$. Since the play output $m_i(t)$ represents the state of the play operator P_{r_i} at the time instant t, the vector $\mathbf{m}(0)$ stands for the initial state of the PI operator.

Assume that the reference signal $y_r(t)$ is a sinusoid

$$y_r(t) = A_{y_r}\sin(\omega t). \qquad (2)$$

Assume also that the input $u(t)$ of the PI operator Γ has an amplitude A_u larger than the largest play radius r_N, which ensures a contraction property for the play operators and enables the independence of the $2\pi/\omega$-periodic steady-state output of the PI operator from its initial state (Tan & Khalil, 2009). The objective of this paper is to compute the steady-state responses of $u(t)$, $m(t)$ and $y(t)$ in Fig. 1 under the sinusoidal reference $y_r(t)$ in (2).

3. The proposed IHB-based approach

This section proposes the IHB-based approach for the harmonic analysis of the system in Fig. 1.

$$\begin{aligned}\Upsilon(t) \triangleq\ & \underbrace{A_{y_r}\sin(\omega t)}_{\triangleq \Upsilon_1(t)} - \underbrace{\sum_{n=1}^{N_H}\frac{A_{u_n}}{|L_1(jn\omega)|}\sin\left[n\omega t+\phi_{u_n}-\underline{/L_1(jn\omega)}\right]}_{\triangleq \Upsilon_2(t)} - \underbrace{\sum_{n=1}^{N_H}\frac{\Delta A_{u_n}}{|L_1(jn\omega)|}\sin\left[n\omega t+\Delta\phi_{u_n}-\underline{/L_1(jn\omega)}\right]}_{\triangleq \Upsilon_3(t)}\\ & - \underbrace{\sum_{n=1}^{N_H}\sum_{i=0}^{N}\theta_i A^i_{m_n}|L_2(jn\omega)|\sin\left[n\omega t+\phi^i_{m_n}+\underline{/L_2(jn\omega)}\right]}_{\triangleq \Upsilon_4(t)} - \underbrace{\sum_{n=1}^{N_H}\sum_{i=0}^{N}\theta_i P'_{r_i}[u;\, m_i(0)](t)\Delta A_{u_n}|L_2(jn\omega)|\sin\left[n\omega t+\Delta\phi_{u_n}+\underline{/L_2(jn\omega)}\right]}_{\triangleq \Upsilon_5(t)}\\ \triangleq\ & \sum_{n=1}^{5}\Upsilon_n(t)=0. \end{aligned} \tag{9}$$

Box I.

3.1. Extension of the IHB method

Under the reference signal $y_r(t)$ in (2), the hysteresis input $u(t)$ is captured by incorporating higher-order harmonics

$$\begin{aligned} u(t) &= \sum_{n=1}^{N_H} A_{u_n}\sin(n\omega t+\phi_{u_n})\\ &= \sum_{n=1}^{N_H}[a_{u_n}\sin(n\omega t)+b_{u_n}\cos(n\omega t)], \end{aligned} \tag{3}$$

where N_H stands for the truncation order of the harmonics, and $a_{u_n} \triangleq A_{u_n}\cos\phi_{u_n}$ and $b_{u_n} \triangleq A_{u_n}\sin\phi_{u_n}$. Note that the DC coefficient A_{u_0} is zero due to the odd symmetry of the PI operator, and is thus not present in (3). Accordingly, define a sufficiently small increment in $u(t)$ as

$$\begin{aligned} \Delta u(t) &= \sum_{n=1}^{N_H}\Delta A_{u_n}\sin(n\omega t+\Delta\phi_{u_n})\\ &= \sum_{n=1}^{N_H}[\Delta a_{u_n}\sin(n\omega t)+\Delta b_{u_n}\cos(n\omega t)], \end{aligned} \tag{4}$$

where $\Delta a_{u_n} \triangleq \Delta A_{u_n}\cos\Delta\phi_{u_n}$ and $\Delta b_{u_n} \triangleq \Delta A_{u_n}\sin\Delta\phi_{u_n}$ with the conditions $|\Delta a_{u_n}| \ll |a_{u_n}|$ and $|\Delta b_{u_n}| \ll |b_{u_n}|$.

The IHB method is an iterative algorithm. At each iteration, the next input is the summation of the current input (3) and the sufficiently small input increment (4). The input increment (4) is computed via an incremental harmonic balance technique introduced in the next subsection. The next input has the same form with the current input (3), since all the involved signals are series of harmonics up to the order N_H. This iteration continues until some convergence criterion is met.

Under the input $u(t)+\Delta u(t)$, expanding the output $m_i(t)$ of the play operator P_{r_i} into a first-order Taylor series, one can obtain

$$P_{r_i}[u+\Delta u;\, m_i(0)](t) \approx P_{r_i}[u;\, m_i(0)](t) + P'_{r_i}[u;\, m_i(0)](t)\Delta u(t) \tag{5}$$

where the symbol $P'_{r_i}[u;\, m_i(0)](t)$ stands for the derivative of the play operator P_{r_i} with respect to its input u, instead of the time variable t (Esbrook et al., 2014). That is,

$$P'_{r_i}[u;\, m_i(0)](t) = \begin{cases} 1, & \text{if } P_{r_i}[u;\, m_i(0)](t) \in \prod_i,\\ 0, & \text{if } P_{r_i}[u;\, m_i(0)](t) \in \prod_i^c. \end{cases} \tag{6}$$

Here $\prod_i$ stands for the boundary region of the play operator P_{r_i}, where $m_i(t) = u(t) \pm r_i$, and $\prod_i^c$ is its complement, namely, the interior region, where $m_i(t)$ is constant.

Two cases are involved in the approximation (5). First, when both $P_{r_i}[u;\, m_i(0)](t)$ and $P_{r_i}[u+\Delta u;\, m_i(0)](t)$ stay in the boundary or interior region, we have a strict equality $P_{r_i}[u+\Delta u;\, m_i(0)](t) = P_{r_i}[u;\, m_i(0)](t) + P'_{r_i}[u;\, m_i(0)](t)\Delta u(t)$. The second case is that one of them is in the interior region while the other is in the boundary region. In this case, the discontinuities of P'_{r_i} at the switching time instants have a negligible impact, because the switching time instants have a Lebesgue measure of zero (Bogachev, 2007), and the input increments are very small, i.e., $|\Delta a_{u_n}| \ll |a_{u_n}|$ and $|\Delta b_{u_n}| \ll |b_{u_n}|$. This statement is also supported by the numerical results in Section 4 later, where the signals $u(t)$, $m(t)$ and $y(t)$ are overlapped with their estimates from the proposed IHB-based approach developed from this approximation.

With the approximation (5) for the play operator, we can obtain the first-order Taylor approximation for the output of the PI operator,

$$\Gamma[u+\Delta u;\, \mathbf{m}(0)](t) \approx \Gamma[u;\, \mathbf{m}(0)](t) + \sum_{i=0}^{N}\theta_i P'_{r_i}[u;\, m_i(0)](t)\Delta u(t). \tag{7}$$

In order to continue the harmonic analysis, we expand the play operator output $m_i(t)$ into N_H harmonics,

$$\begin{aligned} m_i(t) &\approx \sum_{n=1}^{N_H} A^i_{m_n}\sin(n\omega t+\phi^i_{m_n})\\ &= \sum_{n=1}^{N_H}[a^i_{m_n}\sin(n\omega t)+b^i_{m_n}\cos(n\omega t)], \end{aligned} \tag{8}$$

with $a^i_{m_n} \triangleq A^i_{m_n}\cos(\phi^i_{m_n})$ and $b^i_{m_n} \triangleq A^i_{m_n}\sin(\phi^i_{m_n})$. In (8) the superscript ^{i} stands for the variables for the ith play operator. Since the components $L_1(s)$ and $L_2(s)$ are linear systems and satisfy the principle of superposition, a new equation (9) (see Box I) is obtained from $y_r(t) - e(t) - y(t) = 0$. In (9), the second term $\Upsilon_2(t)$ and the third term $\Upsilon_3(t)$ deal with the harmonics in $e(t)$ passing through $L_1(s)$ and generating $u(t)$ in (3) and $\Delta u(t)$ in (4), respectively, while the last two terms $\Upsilon_4(t)$ and $\Upsilon_5(t)$ result from $\Gamma[u+\Delta u;\, \mathbf{m}(0)](t)$ in (7) passing through $L_2(s)$.

The Galerkin's procedure (Fletcher, 2012) is utilized to balance the coefficients on the terms $\sin(n\omega t)$ and $\cos(n\omega t)$ in (9), $n = 1, \ldots, N_H$, i.e., $\Upsilon(t)$ in (9) is required to be orthogonal to the basis functions $\sin(k\omega t)$ and $\cos(k\omega t)$ in the following sense:

$$\int_0^{2\pi}\Upsilon(t)\sin(k\omega t)\mathrm{d}(\omega t) = 0, \tag{10a}$$

$$\int_0^{2\pi}\Upsilon(t)\cos(k\omega t)\mathrm{d}(\omega t) = 0, \tag{10b}$$

$$\frac{A_{u_n}}{|L_1(jn\omega)|}\cos\left[\phi_{u_n} - \underline{/L_1(jn\omega)}\right] + \frac{\Delta A_{u_n}}{|L_1(jn\omega)|}\cos\left[\Delta\phi_{u_n} - \underline{/L_1(jn\omega)}\right] + \sum_{i=0}^{N}\theta_i A^i_{m_n}|L_2(jn\omega)|\cos\left[\phi^i_{m_n} + \underline{/L_2(jn\omega)}\right]$$
$$+\frac{1}{\pi}\sum_{i=0}^{N}\theta_i\sum_{k=1}^{N_H}\int_{\omega t=0}^{2\pi}P'_{r_i}[u;m_i(0)](t)\Delta A_{u_k}|L_2(jk\omega)|\sin\left[k\omega t + \Delta\phi_{u_k} + \underline{/L_2(jk\omega)}\right]\sin(n\omega t)\mathrm{d}(\omega t) = A_{y_r}\delta_{1n}, \tag{12a}$$
$$\frac{A_{u_n}}{|L_1(jn\omega)|}\sin\left[\phi_{u_n} - \underline{/L_1(jn\omega)}\right] + \frac{\Delta A_{u_n}}{|L_1(jn\omega)|}\sin\left[\Delta\phi_{u_n} - \underline{/L_1(jn\omega)}\right] + \sum_{i=0}^{N}\theta_i A^i_{m_n}|L_2(jn\omega)|\sin\left[\phi^i_{m_n} + \underline{/L_2(jn\omega)}\right]$$
$$+\frac{1}{\pi}\sum_{i=0}^{N}\theta_i\sum_{k=1}^{N_H}\int_{\omega t=0}^{2\pi}P'_{r_i}[u;m_i(0)](t)\Delta A_{u_k}|L_2(jk\omega)|\sin\left[k\omega t + \Delta\phi_{u_k} + \underline{/L_2(jk\omega)}\right]\cos(n\omega t)\mathrm{d}(\omega t) = 0. \tag{12b}$$

Box II.

with $k = 1, \ldots, N_H$. With the orthogonality property of the trigonometric functions,

$$\int_0^{2\pi}\sin(ix)\sin(jx)\mathrm{d}x = \begin{cases}0, & \text{if } i \neq j,\\ \pi, & \text{if } i = j,\end{cases} \tag{11a}$$
$$\int_0^{2\pi}\cos(ix)\cos(jx)\mathrm{d}x = \begin{cases}0, & \text{if } i \neq j,\\ \pi, & \text{if } i = j,\end{cases} \tag{11b}$$
$$\int_0^{2\pi}\sin(ix)\cos(jx)\mathrm{d}x = 0, \quad \forall i, j, \tag{11c}$$

we have

$$\int_0^{2\pi}\Upsilon_1(t)\sin(k\omega t)\mathrm{d}(\omega t) = \pi A_{y_r}\delta_{1n},$$
$$\int_0^{2\pi}\Upsilon_1(t)\cos(k\omega t)\mathrm{d}(\omega t) = 0,$$

where δ_{ij} is a Kronecker delta function, that is, $\delta_{ij} = 1$, if $i = j$; otherwise, $\delta_{ij} = 0$. The calculation on the term $\Upsilon_2(t)$ is

$$\int_0^{2\pi}\Upsilon_2(t)\sin(k\omega t)\mathrm{d}(\omega t)$$
$$= \int_0^{2\pi}\sum_{n=1}^{N_H}\frac{A_{u_n}}{|L_1(jn\omega)|}\left\{\sin(n\omega t)\cos\left[\phi_{u_n} - \underline{/L_1(jn\omega)}\right] + \cos(n\omega t)\sin\left[\phi_{u_n} - \underline{/L_1(jn\omega)}\right]\right\}\sin(k\omega t)\mathrm{d}(\omega t)$$
$$= \frac{\pi A_{u_n}}{|L_1(jn\omega)|}\cos\left[\phi_{u_n} - \underline{/L_1(jn\omega)}\right],$$
$$\int_0^{2\pi}\Upsilon_2(t)\cos(k\omega t)\mathrm{d}(\omega t)$$
$$= \int_0^{2\pi}\sum_{n=1}^{N_H}\frac{A_{u_n}}{|L_1(jn\omega)|}\left\{\sin(n\omega t)\cos\left[\phi_{u_n} - \underline{/L_1(jn\omega)}\right] + \cos(n\omega t)\sin\left[\phi_{u_n} - \underline{/L_1(jn\omega)}\right]\right\}\cos(k\omega t)\mathrm{d}(\omega t)$$
$$= \frac{\pi A_{u_n}}{|L_1(jn\omega)|}\sin\left[\phi_{u_n} - \underline{/L_1(jn\omega)}\right].$$

The terms $\Upsilon_3(t)$ and $\Upsilon_4(t)$ share the similar derivation, while the integrals on $\Upsilon_5(t)$ simply hold. The final update from (10) is shown in (12) (see Box II) for $n = 1, 2, \ldots, N_H$.

3.2. Solution of input increments

Given the current input $u(t)$ in (3), the unknown input increment $\Delta u(t)$ in (4) has to be calculated to update $u(t)$. The main challenge in solving (12) for the unknown parameters ΔA_{u_n} and $\Delta\phi_{u_n}$ consisting the input increment $\Delta u(t)$ is the calculation of the unknown harmonic parameters $A^i_{m_n}$ and $\phi^i_{m_n}$ in (8) and $P'_{r_i}[u;m_i(0)](t)$ in (5) for a known multi-harmonic sinusoid $u(t)$ in (3). In order to calculate these quantities from $u(t)$, we have to access the time instants when the play operator switches between the boundary and interior regions. For this purpose, the alternative definition of the play operator in Esbrook and Tan (2012) is utilized. The output $m_i(t)$ of the play operator P_{r_i} is described as

$$m_i(t) = \left[u(t) + P^i_1(t)\right]P^i_2(t) + P^i_3(t),$$

where the pulse wave signals P^i_1, P^i_2 and P^i_3 are defined as

$$P^i_1(t) = -r_i\{\mathrm{sgn}[\dot{u}(t)]\},$$
$$P^i_2(t) = \begin{cases}0, & t \in [t^i_{j_0}, t^i_{j_1}),\\ 1, & t \in [t^i_{j_1}, t^i_{(j+1)_0}),\end{cases}$$
$$P^i_3(t) = \begin{cases}u(t^i_{j_0}) + r_i\left\{\mathrm{sgn}[\dot{u}(t^{i-}_{j_0})]\right\}, & t \in [t^i_{j_0}, t^i_{j_1}),\\ 0, & t \in [t^i_{j_1}, t^i_{(j+1)_0}),\end{cases}$$

with $j = 1, 2, \ldots$. The symbols $t^i_{j_0}$ and $t^i_{j_1}$ are defined as follows. First, assume that under the initial state of $u(t)$, all play operators are in the boundary region. Then, the time instant $t^i_{j_0}$ represents the time instant when the output $m_i(t)$ of the play operator P_{r_i} exits from a boundary region and goes into the interior region, that is Eqs. (12a) and (12b) are given in Box II,

$$u'(t^i_{j_0}) = 0, \ \mathrm{sgn}(u'(t^{i-}_{j_0})) \neq \mathrm{sgn}(u'(t^{i+}_{j_0})), \ t^i_{j_0} > t^i_{(j-1)_1}, \tag{13}$$

and $t^i_{j_1}$ is the time instant that the play operator P_{r_i} moves out of the interior region, which can be divided into two cases. The first one is that the play operator exits from the boundary region opposite from the one that it entered, namely,

$$|u(t^i_{j_0}) - u(t^i_{j_1})| \geq 2r_i, \ t^i_{j_1} \geq t^i_{j_0}. \tag{14}$$

Another one is that the play operator P_{r_i} exists from the same boundary region as the one that it entered, namely,

$$\mathrm{sgn}(\dot{u}(t^{i+}_{j_0}))u(t^i_{j_1}) < \mathrm{sgn}(\dot{u}(t^{i+}_{j_0}))u(t^i_{j_0}), \ t^i_{j_1} \geq t^i_{j_0}. \tag{15}$$

Note that the calculation of the switching time instant series t^i_{j0} and t^i_{j1} is strongly based on the detailed values of $u(t)$, and has to be numerical. Given the discrete time series for one sinusoidal period, the time instants t^i_{j0} and t^i_{j1} satisfying (13)–(15) are searched by a bisection method (Esbrook & Tan, 2012).

During one period $t \in [0, 2\pi/\omega]$, denote $t^i_0 \triangleq 0$ and $t^i_{M+1} \triangleq 2\pi/\omega$, and define t^i_j as the time instant when the play operator P_{r_i} switches between the interior and boundary regions. Define

$H(t_j^i)$ as the derivative of the play operator P_{r_i} in the time interval $[t_j^i, t_{j+1}^i]$,

$$H(t_j^i) = \begin{cases} 1, & \text{if } \forall t \in [t_j^i, t_{j+1}^i),\ P_{r_i}[u; m_i(0)](t) \in \prod_i, \\ 0, & \text{if } \forall t \in [t_j^i, t_{j+1}^i),\ P_{r_i}[u; m_i(0)](t) \in \prod_i^c, \end{cases} \tag{16}$$

where $i = 0, 1, \ldots, N$, and $j = 0, 1, 2, \ldots, M$. After necessary cosine expansion deduction from (12), we can derive a linear matrix equality

$$\begin{bmatrix} C_{11} & C_{12} \\ C_{21} & C_{22} \end{bmatrix} \begin{bmatrix} \Delta a_u \\ \Delta b_u \end{bmatrix} = \begin{bmatrix} R_1 \\ R_2 \end{bmatrix}. \tag{17}$$

Here $\Delta a_u \triangleq [\Delta a_{u_1}, \cdots, \Delta a_{u_{N_H}}]^T$, and $\Delta b_u \triangleq [\Delta b_{u_1}, \cdots, \Delta b_{u_{N_H}}]^T$. The (n, k)th element of the square coefficient matrix C_{ij}, denoted as $C_{ij}(n, k)$, is obtained as

$$\begin{aligned} C_{11}(n,k) &= \frac{1}{\pi}\sum_{i=0}^{N}\theta_i \sum_{m=0}^{M} H(t_m^i)[A_{kn}^i(T_m^i, T_{m+1}^i)a_{L_2}(k) \\ &\quad + B_{kn}^i(T_m^i, T_{m+1}^i)b_{L_2}(k)] + a_{L_1}^-(n)\delta_{nk}, \\ C_{12}(n,k) &= \frac{1}{\pi}\sum_{i=0}^{N}\theta_i \sum_{m=0}^{M} H(t_m^i)[B_{kn}^i(T_m^i, T_{m+1}^i)a_{L_2}(k) \\ &\quad - A_{kn}^i(T_m^i, T_{m+1}^i)b_{L_2}(k)] + b_{L_1}^-(n)\delta_{nk}, \\ C_{21}(n,k) &= \frac{1}{\pi}\sum_{i=0}^{N}\theta_i \sum_{m=0}^{M} H(t_m^i)[B_{nk}^i(T_m^i, T_{m+1}^i)a_{L_2}(k) \\ &\quad + C_{kn}^i(T_m^i, T_{m+1}^i)b_{L_2}(k)] - b_{L_1}^-(n)\delta_{nk}, \\ C_{22}(n,k) &= \frac{1}{\pi}\sum_{i=0}^{N}\theta_i \sum_{m=0}^{M} H(t_m^i)[C_{kn}^i(T_m^i, T_{m+1}^i)a_{L_2}(k) \\ &\quad - B_{nk}^i(T_m^i, T_{m+1}^i)b_{L_2}(k)] + a_{L_1}^-(n)\delta_{nk}, \end{aligned}$$

where $T_m^i \triangleq \omega t_m^i$, $a_{L_1}^-(n) \triangleq \cos(\underline{/L_1(jn\omega)})/|L_1(jn\omega)|$, $b_{L_1}^-(n) \triangleq \sin(\underline{/L_1(jn\omega)})/|L_1(jn\omega)|$, $a_{L_2}(n) \triangleq |L_2(jn\omega)| \cos(\underline{/L_2(jn\omega)})$, and $b_{L_2}(n) \triangleq |L_2(jn\omega)| \sin(\underline{/L_2(jn\omega)})$. The symbols A_{nk}^i, B_{nk}^i and C_{nk}^i are expressed as

$$\begin{aligned} A_{nk}^i(T_m^i, T_{m+1}^i) &= \int_{T_m^i}^{T_{m+1}^i} \sin(nt)\sin(kt)\mathrm{d}t, \\ B_{nk}^i(T_m^i, T_{m+1}^i) &= \int_{T_m^i}^{T_{m+1}^i} \cos(nt)\sin(kt)\mathrm{d}t, \\ C_{nk}^i(T_m^i, T_{m+1}^i) &= \int_{T_m^i}^{T_{m+1}^i} \cos(nt)\cos(kt)\mathrm{d}t. \end{aligned}$$

The nth elements in the vectors R_1 and R_2 are, respectively,

$$\begin{aligned} R_1(n) &= -\sum_{i=1}^{N}\theta_i\left[a_{m_n}^i a_{L_2}(n) - b_{m_n}^i b_{L_2}(n)\right] - a_{u_n} a_{L_1}^-(n) \\ &\quad - b_{u_n} b_{L_1}^-(n) + A_{y_r}\delta_{1n}, \\ R_2(n) &= -\sum_{i=1}^{N}\theta_i\left[a_{m_n}^i b_{L_2}(n) + b_{m_n}^i a_{L_2}(n)\right] + a_{u_n} b_{L_1}^-(n) \\ &\quad - b_{u_n} a_{L_1}^-(n). \end{aligned}$$

The derivation of (17) from (12) is presented in Appendix B.

3.3. Steps of the IHB-based approach

The IHB-based approach is composed by the following steps.

Outer loop for $N_H = 1, 2, 3, \ldots$

Step A. Estimate $u(t)$ in (3) as $\hat{u}^{N_H}(t)$, consisting of the first N_H-order harmonics, in the following inner loop.

Inner loop for $k = 1, 2, \ldots$ until convergence.

Step 1. If $N_H = 1$, evaluate $\hat{u}^{N_H,0}(t)$ as the solution from the DFM and stop; otherwise, initialize $\hat{u}^{N_H,0}(t)$ as the solution $\hat{u}^{N_H-1}(t)$ from the IHB-based approach at the last outer-loop iteration.

Step 2. Calculate the harmonic approximation at the kth inner-loop iteration of the hysteresis output $m_i(t)$ in (8) as $\hat{m}_i^{N_H,k}(t)$ via (19) (replacing $\hat{u}(t)$ therein by $\hat{u}^{N_H,k}(t)$) and the derivative $H(t_j^i)$ in (16) as $\hat{H}^{N_H,k}(t_j^i)$, and compute the increment $\Delta u(t)$ in (4) from (17) as $\Delta\hat{u}^{N_H,k}(t)$.

Step 3. Update the hysteresis input as $\hat{u}^{N_H,k+1}(t) = \hat{u}^{N_H,k}(t) + \Delta\hat{u}^{N_H,k}(t)$. If the maximum value of $\Delta\hat{a}_{u_n}^{N_H,k}$ and $\Delta\hat{b}_{u_n}^{N_H,k}$ $(n = 1, 2, \ldots, N_H)$ is smaller than a given threshold ε_0, then evaluate $\hat{u}^{N_H}(t) = \hat{u}^{N_H,k}(t)$ and stop; otherwise, set $k = k + 1$ and go to Step 2.

End of inner loop

Step B. Calculate the fitness value between the two adjacent estimation $\hat{u}^{N_H}(t)$ and $\hat{u}^{N_H+1}(t)$

$$F(N_H) = \left(1 - \frac{\|\hat{u}^{N_H} - \hat{u}^{N_H+1}\|}{\|\hat{u}^{N_H+1} - E\{\hat{u}^{N_H+1}\}\|}\right) \times 100\%.$$

where $\|\cdot\|$ and $E\{\cdot\}$ stand for the 2−norm and the mean value of the operand, respectively.

Step C. If the difference between two adjacent fitness values $|F(N_H+1) - F(N_H)|$ is less than a given threshold ε_{F0}, then evaluate $\hat{u}(t) = \hat{u}^{N_H}(t)$ and stop; otherwise, set $N_H = N_H + 1$ and go to Step A.

Step D. Calculate the high-order estimates of $y(t)$ and $m(t)$ by

$$\hat{y}(t) = A_{y_r}\sin(\omega t) - \sum_{n=1}^{N_H} \frac{\hat{A}_{u_n}}{|L_1(jn\omega)|}\sin\left[n\omega t + \hat{\phi}_{u_n} - \underline{/L_1(jn\omega)}\right] \tag{18}$$

$$\begin{aligned} \hat{m}(t) = &\frac{A_{y_r}}{|L_1(j\omega)|}\sin[\omega t - \underline{/L_1(j\omega)}] - \sum_{n=1}^{N_H}\frac{\hat{A}_{u_n}}{|L_1(jn\omega)||L_2(jn\omega)|} \\ &\times \sin\left[n\omega t + \hat{\phi}_{u_n} - \underline{/L_1(jn\omega)} - \underline{/L_2(jn\omega)}\right]. \end{aligned} \tag{19}$$

End of outer loop

Here the two thresholds ε_0 and ε_{F0}, which terminate the inner and outer loops, respectively, are subject to the users' design.

4. Numerical results

A numerical example is provided to illustrate the effectiveness of the proposed IHB-based approach, and make a comparison with the DFM.

In this example, the reference signal is assumed to be $y_r(t) = \sin(\pi t/10)$, and the linear part $L_2(s)$ is $L_2(s) = 1/(8s + 1)$. The linear component $L_1(s)$ represents a proportional–integral controller, obtained based on the internal model control rule (Aström & Hägglund, 2006) with closed-loop time constant $\tau_C = 2$ s, namely, $L_1(s) = 4(1 + 1/8s)$. Note that the proposed approach

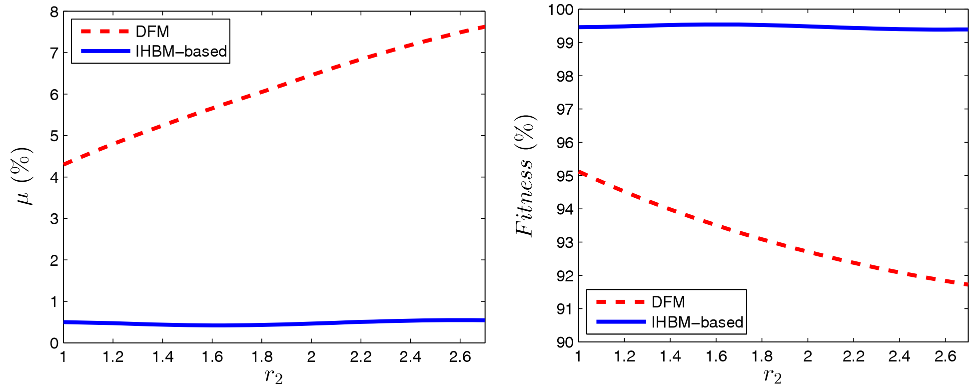

Fig. 2. The performance indices μ (left) and *Fitness* (right) calculated from the DFM and the IHB-based approach.

Table 1
Harmonic amplitudes a_{u_n}, b_{u_n}, a_{m_n}, b_{m_n}, a_{y_n} and b_{y_n} from DFM and the IHB-based approach compared with the actual values from spectrum analysis.

Coef.	Actual	DFM	Error (%)	IHB	Error (%)
a_{u_1}	4.0868	3.8889	4.8424	4.0844	0.0587
b_{u_1}	2.9554	3.2062	−8.4862	2.9518	0.1218
a_{u_3}	−0.1020			−0.1031	−1.0784
b_{u_3}	0.2007			0.1990	0.8470
a_{m_1}	2.8552	3.0145	−5.5793	2.8547	0.0175
b_{m_1}	0.5795	0.6981	−20.4659	0.5753	0.7248
a_{m_3}	0.3765			0.3752	0.3453
b_{m_3}	0.1957			0.1943	0.7154
a_{y_1}	0.4278	0.4791	−11.9916	0.4289	−0.2571
b_{y_1}	−0.7732	−0.8071	−4.3844	−0.7721	0.1423
a_{y_3}	0.0244			0.0246	−0.8197
b_{y_3}	−0.0375			−0.0372	0.0080

is applicable to general linear controllers, not confined to the proportional–integral controller here. The PI operator consists of three play operators, where $\mathbf{r} = [0, 1, r_2]^T$ and $\boldsymbol{\theta} = [0.1, 0.1, 0.8]^T$. The variable r_2 is a good indicator of the hysteresis severity for the closed-loop system, since as r_2 increases, the hysteresis width increases. The interval for the parameter r_2 is chosen as $[1, 2.7]$. For the IHB-based approach, we set the two thresholds as $\varepsilon_0 = 10^{-8} \max\{\|\hat{a}_{u_n}^{N_H,k}\|, \|\hat{b}_{u_n}^{N_H,k}\|\}$ and $\varepsilon_{F0} = 10^{-8}$.

Define two indices for quantifying the performances of the IHB-based approach

$$\mu = \frac{E(|\hat{u} - u|)}{E(|u|)} \times 100\%, \tag{20a}$$

$$Fitness = \left(1 - \frac{\|\hat{u} - u\|}{\|u - E\{u\}\|}\right) \times 100\%. \tag{20b}$$

Here, $\hat{u}$ is the estimation of hysteresis input from the IHB-based approach, and u is the one from the simulation.

The IHB-based approach stops at $N_H = 9$. The average iteration number of the inner loop in the IHB-based approach for $N_H = 9$ is 26 in this example, which indicates that the computation cost is minor, even if the thresholds ε_0 and ε_{F0} are tight. The performance indices in (20) for the IHB-based approach are shown in Fig. 2; as a comparison, the counterparts of the DFM are given, too. This figure reveals that the IHB-based approach yields more accurate estimation of $u(t)$ than the DFM; moreover, the IHB-based approach is more robust to the parameter r_2, while the DFM degrades as r_2 increases.

As a further investigation, the estimates of $u(t)$, $m(t)$ and $y(t)$ from the DFM and the IHB-based approach for the case $r_2 = 2.7$ are plotted in Fig. 3. The estimates $\hat{u}(t)$, $\hat{m}(t)$ and $\hat{y}(t)$ from the IHB-based approach perfectly overlays with the actual signals $u(t)$, $m(t)$ and $y(t)$, respectively, while the estimates from the DFM have clear differences from the actual ones. Table 1 quantitatively compares the lower-order harmonic amplitudes a_{u_n} and b_{u_n} of $u(t)$, a_{m_n} and b_{m_n} of $m(t)$, and a_{y_n} and b_{y_n} of $y(t)$ from the DFM and IHB-based approach with the actual values from the spectrum analysis using Fourier transform. The percent error is calculated using the formulation: (Actual–Estimated)/Actual. In Table 1, the DFM has percentage errors 4.8% and 8.5% in estimating the fundamental harmonic components a_{u_1} and b_{u_1}, while the IHB-based approach greatly reduces them to only 0.06% and 0.12%. Table 1 also reveals that the IHB-based approach has good estimation for the third-order harmonic component, which is also not ignorable because $|a_{u_3}/a_{u_1}| = 2.4958\%$ and $|b_{u_3}/b_{u_1}| = 6.7910\%$. The DFM also exits much larger percentage errors in estimating a_{m_1}, b_{m_1}, a_{y_1} and b_{y_1} than the IHB-based approach, due to the usage of only the fundamental harmonics. This example proves that the IHB-based approach is much more accurate than the DFM in dealing with strong hysteresis nonlinearity.

5. Conclusions

In this paper, the IHB-based approach was proposed for the harmonic analysis of closed-loop systems with the PI operator. Compared with the traditional DFM, the proposed approach is able to capture the harmonics up to an arbitrary order; hence, excellent approximation can be achieved even for systems with strong hysteresis, where the DFM deteriorates considerably due to the presence of significant high-order harmonics.

The proposed IHB-based approach is not limited to the PI operator; thus, one future work is to extend the approach to the analysis of the forced multi-frequency response of systems with a general class of hysteresis operators consisting of superposition of multiple elementary operators. This work is a prerequisite for many subsequent studies, such as analyzing the effects of sticky control valves on the control performance of feedback control systems. Another future work is to investigate how modeling errors of hysteresis would affect the harmonic analysis results, since obtaining an accurate hysteresis model is rather difficult in practice and it is necessary to have a solution not overly dependent on the model accuracy.

Appendix A. Describing function method

The describing function method (DFM) is briefly revisited here (Gelb & Velde, 1968). The describing function (DF) N_i for a

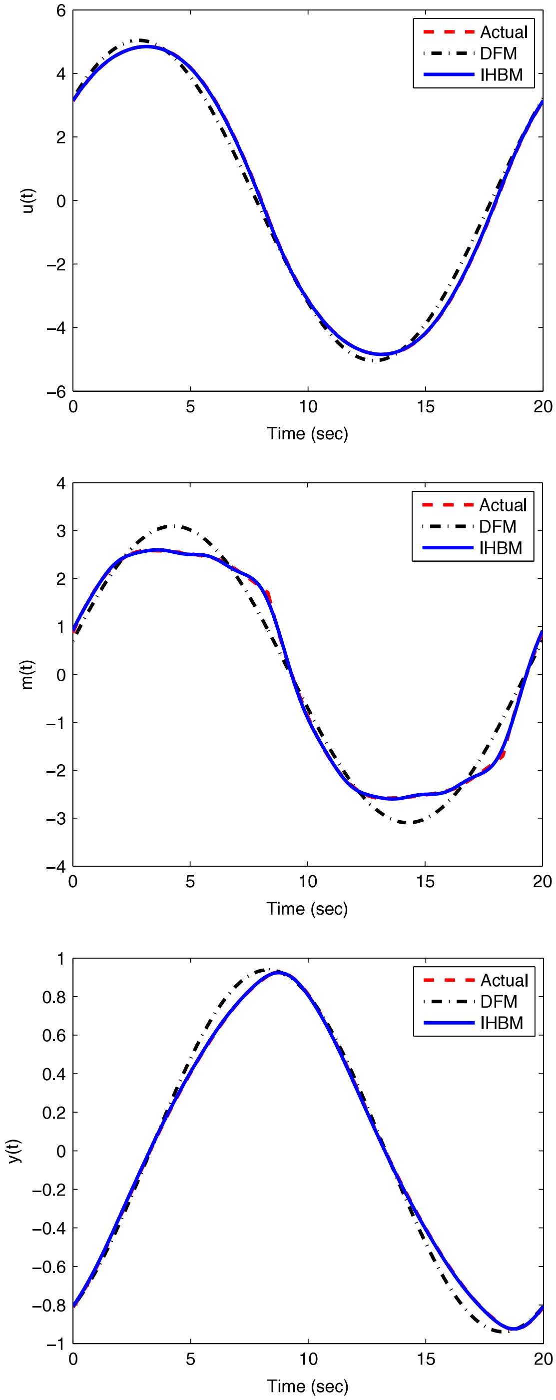

Fig. 3. The comparison of the estimated $u(t)$ (upper), $m(t)$ (middle) and $y(t)$ (bottom) from the DFM and the IHB-based approach for $r_2 = 2.7$.

play operator P_{r_i} having the play radius r_i is given by

$$|N_i(A)| = \frac{1}{A}\sqrt{a_{1_i}^2 + b_{1_i}^2}, \ \underline{/N_i(A)} = \arctan\left(\frac{a_{1_i}}{b_{1_i}}\right),$$

where A is the amplitude of the sinusoidal input of the play operator P_{r_i}, and the fundamental harmonic coefficients a_{1_i} and b_{1_i} are

$$a_{1_i} = \frac{4r_i}{\pi}\left(\frac{r_i}{A} - 1\right), \ b_{1_i} = \frac{A}{\pi}\left[\frac{\pi}{2} - \arcsin(x_i) - x_i\sqrt{1 - x_i^2}\right],$$

with $x_i \triangleq 2r_i/A - 1$. Then, the DF for a PI operator in (1) is a superposition of the DFs of its elementary play operators, namely,

$$N(A) = \sum_{i=0}^{N} \theta_i \mathrm{Re}\left\{|N_i(A)|e^{j\underline{/N_i(A)}}\right\}. \tag{A.1}$$

The DFM approximates $u(t)$ as $u(t) = A_u \sin(\omega t + \phi_u)$. Because the linear subsystems $L_1(s)$ and $L_2(s)$ have well-defined frequency responses, an equality is formulated from $y_r(t) - e(t) = y(t)$

together with (A.1) for the fundamental harmonic component as

$$A_{y_r}\sin(\omega t)-\frac{A_u}{|L_1(j\omega)|}\sin\left[\omega t+\phi_u-\angle L_1(j\omega)\right]$$
$$=\sum_{i=0}^{N}A_u\theta_i|N_i(A_u)||L_2(j\omega)|\sin\left[\omega t+\phi_u+\angle N_i(A_u)+\angle L_2(j\omega)\right],$$

which gives two equalities in terms of the coefficients of $\sin(\omega t)$ and $\cos(\omega t)$, uniquely determining the two unknowns A_u and ϕ_u,

$$A_{y_r}-\frac{A_u}{|L_1(j\omega)|}\cos\left[\phi_u-\angle L_1(j\omega)\right]$$
$$-\sum_{i=0}^{N}A_u\theta_i|N_i(A_u)||L_2(j\omega)|\cos\left[\phi_u+\angle N_i(A_u)+\angle L_2(j\omega)\right]=0,$$

$$\frac{A_u}{|L_1(j\omega)|}\sin\left[\phi_u-\angle L_1(j\omega)\right]$$
$$+\sum_{i=0}^{N}A_u\theta_i|N_i(A_u)||L_2(j\omega)|\sin\left[\phi_u+\angle N_i(A_u)+\angle L_2(j\omega)\right]=0.$$

It is clear that a numerical method, for example, the Newton–Raphson algorithm (Atkinson, 2008), is required to solve these two nonlinear equations for A_u and ϕ_u.

Appendix B. Complementary calculation details

The derivation from (12) to (17) is expanded here. With the notations beneath (17), the first left-side term of (12a) becomes

$$\begin{aligned}&\frac{A_{u_n}}{|L_1(jn\omega)|}\cos\left[\phi_{u_n}-\angle L_1(jn\omega)\right]\\&=A_{u_n}\cos\phi_{u_n}\frac{\cos\angle L_1(jn\omega)}{|L_1(jn\omega)|}+A_{u_n}\sin\phi_{u_n}\frac{\sin\angle L_1(jn\omega)}{|L_1(jn\omega)|}\\&=a_{u_n}a^-_{L_1}(n)+b_{u_n}b^-_{L_1}(n).\end{aligned}\tag{B.1}$$

Similarly, the second and third left-side terms of (12a) are

$$\begin{aligned}&\frac{\Delta A_{u_n}}{|L_1(jn\omega)|}\cos\left[\Delta\phi_{u_n}-\angle L_1(jn\omega)\right]\\&\qquad=\Delta a_{u_n}a^-_{L_1}(n)+\Delta b_{u_n}b^-_{L_1}(n),\end{aligned}\tag{B.2}$$

$$\begin{aligned}&\sum_{i=0}^{N}\theta_iA^i_{m_n}|L_2(jn\omega)|\cos\left[\phi^i_{m_n}+\angle L_2(jn\omega)\right]\\&\qquad=\sum_{i=0}^{N}\theta_i\left[a^i_{m_n}a_{L_2}(n)-b^i_{m_n}b_{L_2}(n)\right].\end{aligned}\tag{B.3}$$

With the definition $H(t^i_j)$ in (16), the integral component of the fourth left-side term of (12a) yields

$$\begin{aligned}&\int_{\omega t=0}^{2\pi}P'_{r_i}[u;m_i(0)](t)\Delta A_{u_k}|L_2(jk\omega)|\sin\left[k\omega t+\Delta\phi_{u_k}\right.\\&\quad\left.+\angle L_2(jk\omega)\right]\sin(n\omega t)\mathrm{d}(\omega t)\\&=\sum_{m=0}^{M}H(t^i_m)\int_{t=t^i_m}^{t^i_{m+1}}\Delta A_{u_k}|L_2(jk\omega)|\sin\left[k\omega t+\Delta\phi_{u_k}+\angle L_2(jk\omega)\right]\\&\quad\times\sin(n\omega t)\mathrm{d}(\omega t)\\&=\sum_{m=0}^{M}H(t^i_m)\int_{t=t^i_m}^{t^i_{m+1}}\Delta A_{u_k}|L_2(jk\omega)|\left[\sin(k\omega t+\Delta\phi_{u_k})\right.\\&\quad\left.\times\cos\angle L_2(jk\omega)+\cos(k\omega t+\Delta\phi_{u_k})\sin\angle L_2(jk\omega)\right]\sin(n\omega t)\mathrm{d}(\omega t)\\&=\sum_{m=0}^{M}H(t^i_m)\int_{t=t^i_m}^{t^i_{m+1}}\Delta A_{u_k}\left\{\left[\sin(k\omega t)\cos\Delta\phi_{u_k}+\cos(k\omega t)\sin\Delta\phi_{u_k}\right]\right.\\&\quad\times a_{L_2}(k)+\left[\cos(k\omega t)\cos\Delta\phi_{u_k}-\sin(k\omega t)\sin\Delta\phi_{u_k}\right]b_{L_2}(k)\left.\right\}\\&\quad\times\sin(n\omega t)\mathrm{d}(\omega t)\\&=\sum_{m=0}^{M}H(t^i_m)\left[A^i_{kn}(T^i_m,T^i_{m+1})a_{L_2}(k)+B^i_{kn}(T^i_m,T^i_{m+1})b_{L_2}(k)\right]\Delta a_{n_k}\\&\quad+\left[B^i_{kn}(T^i_m,T^i_{m+1})a_{L_2}(k)-A^i_{kn}(T^i_m,T^i_{m+1})b_{L_2}(k)\right]\Delta b_{n_k}.\end{aligned}\tag{B.4}$$

The above Eqs. (B.1)–(B.4) is finally reformulated in a matrix manner as

$$\begin{bmatrix}C_{11} & C_{12}\end{bmatrix}\begin{bmatrix}\Delta a_u\\ \Delta b_u\end{bmatrix}=R_1.$$

The calculation for (12b) is completely parallel to the above equations, and is omitted here.

References

Aström, K. J., & Hägglund, T. (2006). *Advanced PID control*. ISA-The Instrumentation, Systems, and Automation Society.

Atkinson, K. E. (2008). *An introduction to numerical analysis*. John Wiley & Sons.

Bertotti, G., & Mayergoyz, I. D. (Eds.). (2005). *The science of hysteresis Volume I, II and III*. Academic Press.

Bogachev, V. I. (2007). *Measure theory*. Springer-Verlag.

Brokate, M., & Sprekels, J. (1996). *Hysteresis and phase transitions*. Springer-Verlag.

Cavallo, A., Natale, S., abd Pirozzi, C., & Visone, C. (2005). Limit cycles in control systems employing smart actuators with hysteresis. *IEEE/ASME Transactions on Mechatronics*, *10*(2), 172–180.

Chen, X., Hisayama, T., & Su, C. Y. (2009). Pseudo-inverse-based adaptive control for uncertain discrete time systems preceded by hysteresis. *Automatica*, *45*(2), 469–476.

Chen, Y., Liu, J., & Meng, G. (2012). Incremental harmonic balance method for nonlinear flutter of an airfoil with uncertain-but-bounded parameters. *Applied Mathematical Modelling*, *36*(2), 657–667.

Chen, J., Ren, B., & Zhong, Q. C. (2016). UDE-based trajectory tracking control of piezoelectric stages. *IEEE Transactions on Industrial Electronics*, *63*(10), 6450–6459.

Choudhury, M. A. A. S., Shah, S. L., & Thornhill, N. F. (2008). *Diagnosis of process nonlinearities and valve stiction: data driven approaches*. Springer-Verlag.

Cuadros, M. A. S. L., Munaro, C. J., & Munareto, S. (2012). Improved stiction compensation in pneumatic control valves. *Computers & Chemical Engineering*, *38*, 106–114.

Edardar, M., Tan, X., & Khalil, H. K. (2014). Tracking error analysis for feedback systems with hysteresis inversion and fast linear dynamics. *Journal of Dynamic Systems, Measurement, and Control*, *136*(4), 041010 (12 pp).

Esbrook, A., & Tan, X. (2012). Harmonic analysis for hysteresis operators with application to control design for systems with hysteresis. In *2012 amer. control conf.* (pp. 1652–1657).

Esbrook, A., Tan, X., & Khalil, H. K. (2014). Self-excited limit cycles in an integral-controlled system with backlash. *IEEE Transactions on Automatic Control*, *59*(4), 1020–1025.

Fang, L., & Wang, J. (2015). Identification of hammerstein systems using preisach model for sticky control valves. *Industrial and Engineering Chemistry Research*, *54*(3), 1028–1040.

Fang, L., Wang, J., & Tan, X. (2016). Frequency response analysis for closed-loop systems with hysteresis using incremental harmonic balance. In *2016 amer. control conf.* (pp. 1305–1310).

Fletcher, C. A. J. (2012). *Computational Galerkin methods*. Springer.

Gelb, A., & Velde, W. E. V. (1968). *Multiple-input describing functions and nonlinear system design*. McGraw-Hill.

Hägglund, T. (2002). A friction compensator for pneumatic control valves. *Journal of Process Control*, *12*(8), 897–904.

Hsu, J. T., & Ngo, K. D. T. (1997). A Hammerstein-based dynamic model for hysteresis phenomenon. *IEEE Transactions on Power Electronics*, *12*(3), 406–413.

Huang, R., Zhang, J., & Zhang, X. (2016). Adaptive tracking control of uncertain switched non-linear systems with application to aircraft wing rock. *IET Control Theory & Applications*, *10*(15), 1755–1762.

Ivan, L. Z. X., & Lakshminarayanan, S. (2009). A new unified approach to valve stiction quantification and compensation. *Industrial and Engineering Chemistry Research*, *48*(7), 3474–3483.

Iyer, R. V., & Tan, X. (2009). Control of hysteretic systems through inverse compensation. *IEEE Control Systems Magazine*, *29*(1), 83–99.

Janaideh, M. A., & Kreji, P. (2013). Inverse rate-dependent Prandtl-Ishlinskii model for feedforward compensation of hysteresis in a piezomicropositioning actuator. *IEEE Transactions on Mechatronics*, *18*(5), 1498–1507.

Janaideh, M. A., Rakheja, S., & Su, C. Y. (2009). A generalized Prandtl-Ishlinskii model for characterizing the hysteresis and saturation nonlinearities of smart actuators. *Smart Materials and Structures*, *18*(4), 045001.

Janaideh, M. A., Rakotondrabe, M., & Tan, X. (2016). Guest editorial focused section on hysteresis in smart mechatronic systems: Modeling, identification, and control. *IEEE Transactions on Mechatronics*, *21*(1), 1–3.
Jelali, M., & Huang, B. (Eds.). (2010). *Detection and diagnosis of stiction in control loops: State of the art and advanced methods*. Springer-Verlag.
Kuhnen, K. (2003). Modeling, identification and compensation of complex hysteretic nonlinearities: A modified Prandtl-Ishlinskii approach. *European Journal of Control*, *9*(4), 407–418.
Liu, S., Su, C. Y., & Li, Z. (2014). Robust adaptive inverse control of a class of nonlinear systems with Prandtl-Ishlinskii hysteresis model. *IEEE Transactions on Automatic Control*, *59*(8), 2170–2175.
Macki, J. W., Nistri, P., & Zecca, P. (1992). Periodic oscillations in systems with hysteresis. *Rocky Mountain Journal of Mathematics*, *22*(2), 669–681.
Mayergoyz, I. D. (2003). *Mathematical models of hysteresis and their applications*. Academic Press.
Mickens, R. E. (1984). Comments on the method of harmonic balance. *Journal of Sound and Vibration*, *94*(3), 456–460.
Mohammad, M., & Huang, B. (2012). Compensation of control valve stiction through controller tuning. *Journal of Process Control*, *22*(9), 1800–1819.
Riccardi, L., Naso, D., Janocha, H., & Turchiano, B. (2012). A precise positioning actuator based on feedback-controlled magnetic shape memory alloys. *Mechatronics*, *22*(5), 568–576.
Riccardi, L., Naso, D., Turchiano, B., & Janocha, H. (2013). Adaptive control of positioning systems with hysteresis based on magnetic shape memory alloys. *IEEE Transactions on Control Systems Technology*, *21*(6), 2011–2023.
Shan, Y., & Leang, K. K. (2012). Accounting for hysteresis in repetitive control design: Nanopositioning example. *Automatica*, *48*(8), 1751–1758.
Shen, Y., Yang, S., & Liu, X. (2006). Nonlinear dynamics of a spur gear pair with time-varying stiffness and backlash based on incremental harmonic balance method. *International Journal of Mechanical Sciences*, *48*(11), 1256–1263.
Smith, R. C. (2005). *Smart material systems: model development*. Society for Industrial and Applied Mathematics.
Tan, X., & Baras, J. S. (2004). Modeling and control of hysteresis in magnetostrictive actuators. *Automatica*, *40*(9), 1469–1480.
Tan, X., & Iyer, R. V. (2009). Modeling and control of hysteresis: Introduction to the special section. *IEEE Control Systems Magazine*, *29*(1), 26–29.
Tan, X., & Khalil, H. K. (2009). Two-time-scale averaging of systems involving operators and its application to adaptive control of hysteretic systems. In *2009 amer. control conf.* (pp. 4476–4481).
Wang, Q., & Su, C. Y. (2006). Robust adaptive control of a class of nonlinear systems including actuator hysteresis with Prandtl-Ishlinskii presentations. *Automatica*, *42*(5), 859–867.
Webb, G. V., Lagoudas, D. C., & Kurdila, A. J. (1998). Hysteresis modeling of SMA actuators for control applications. *Journal of Intelligent Material Systems and Structures*, *9*(6), 432–448.

Lei Fang received the B.E. degree in automatic control from Nanjing University, Nanjing, China, in 2011. He is currently working toward the Ph.D. degree in the College of Engineering, Peking University, Beijing, China. His research interests include system identification and its application to modeling, detection and compensation of control valve stiction in industrial processes.

Jiandong Wang is presently a full Professor of College of Electrical Engineering and Automation at the Shandong University of Science and Technology, Qingdao, Shandong Province, China. He received the B.E. degree in automatic control from Beijing University of Chemical Technology, Beijing, China, in 1997, and the M.Sc and Ph.D. degrees in Electrical and Computer Engineering from the University of Alberta, Canada, in 2003 and 2007, respectively. From 1997 to 2001, he was a Control Engineer with the Beijing Tsinghua Energy Simulation Company, Beijing, China. From February 2006 to August 2006, he was a Visiting Scholar at the Department of System Design Engineering at the Keio University, Japan. From December 2006 to October 2016, he was an assistant/associate/full Professor with the College of Engineering, Peking University, China. His research interests include industrial alarm systems, process monitoring and management, system identification and their applications to industrial problems. Dr. Wang has served as an Associate Editor/Guest Editor for Systems and Control Letters, and Control Engineering Practice.

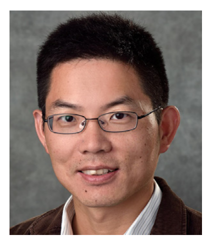

Xiaobo Tan received the B.Eng. and M.Eng. degrees in automatic control from Tsinghua University, Beijing, China, in 1995 and 1998, respectively, and the Ph.D. degree in electrical and computer engineering from the University of Maryland, College Park, in 2002. He is currently an MSU Foundation Professor with the Departments of Electrical and Computer Engineering and Mechanical Engineering at Michigan State University. His research interests include modeling and control of systems with hysteresis, electroactive polymer sensors and actuators, bio-inspired underwater robots and their application to environmental sensing, and soft robotics. He is a Fellow of IEEE.